Science Advances
AAAS

Supplementary Materials for

Augmenting L3MBTL2-induced condensates suppresses tumor growth in osteosarcoma

Li Zhong *et al.*

Corresponding author: Dan Liao, liaodan@sysucc.org.cn; Tiebang Kang, kangtb@sysucc.org.cn; Junqiang Yin, yinjunqiang77@163.com

Sci. Adv. **9**, eadi0889 (2023)
DOI: 10.1126/sciadv.adi0889

The PDF file includes:

Figs. S1 to S10
Legends for tables S1 to S12

Other Supplementary Material for this manuscript includes the following:

Tables S1 to S12

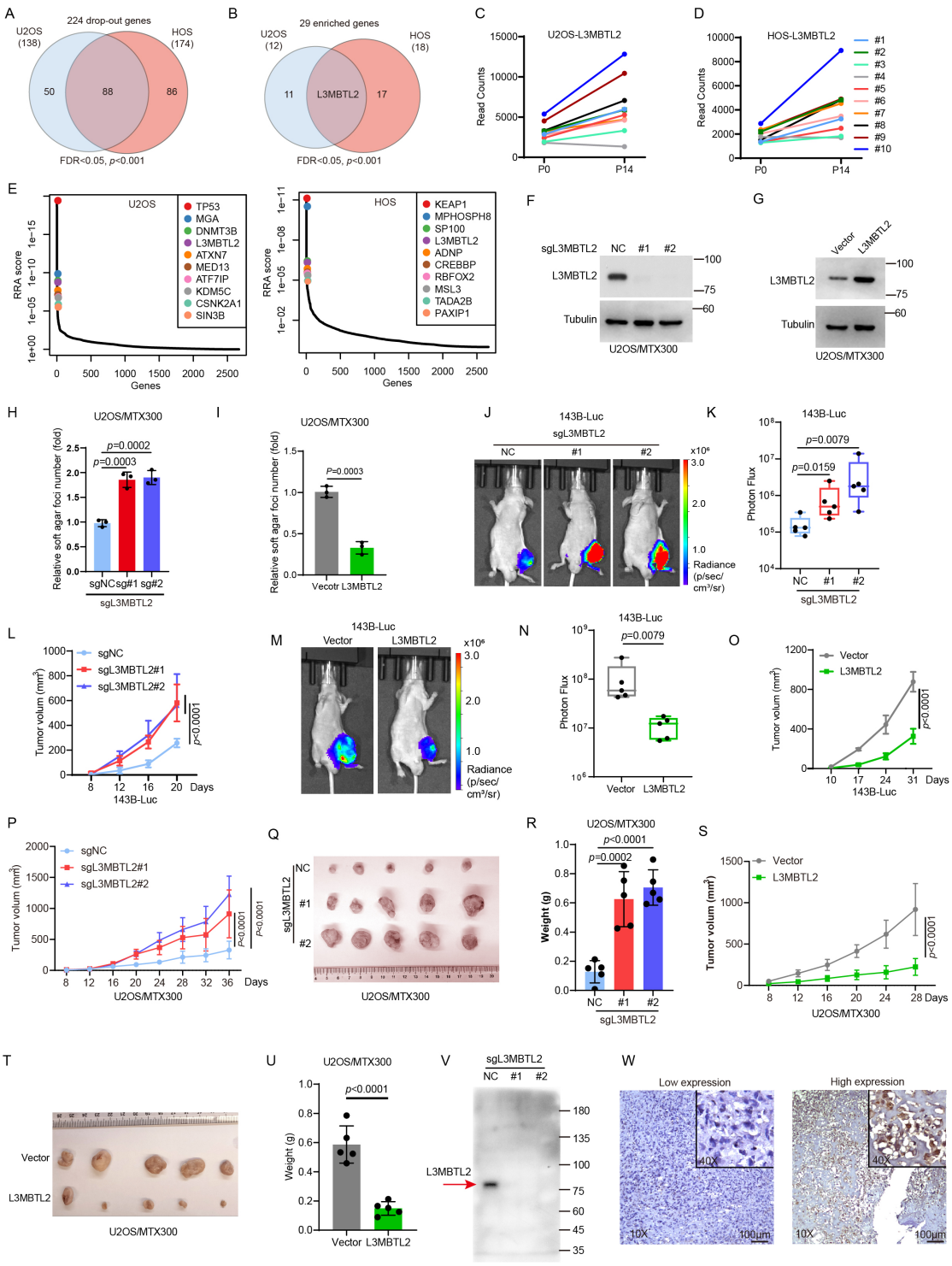

Fig. S1. CRISPR-Cas9 screening reveals that L3MBTL2 functions as a tumor suppressor in osteosarcoma

(**A, B**) Venn diagram shows numbers of dropout genes (**A**) and enriched genes (**B**) at the indicated FDR and *p* values.

(**C, D**) Graphs show read counts of individual sgRNAs targeting L3MBTL2 before and after 14 PD in both U2OS (**C**)and HOS (**D**) cells.

(**E**) Genes significantly enriched after 14 population doubling were identified using the MAGeCK program in the indicated osteosarcoma cell lines. The top 10 enriched genes in this screen are shown. The robust rank aggregation (RPA) algorithm was used to rank sgRNAs based on *p* values.

(**F, G**) The indicated U2OS/MTX300 stable cells were analyzed by Western blotting. Data are representative of n = 3 biologically independent experiments.

(**H, I**) Anchorage-independent assays were performed for the indicated U2OS/MTX300 stable cells. The colony numbers per field were counted. Data are mean ± s.d. of n = 3 biologically independent experiments. *p* values are shown.

(**J-O**) The indicated 143B-Luc stable cells were orthotopically injected into mice. **J and M**. Representative Bioluminescence images of mice at the end point. **K and N**. Automated quantification of bioluminescence images. **L and O**. Tumor growth was measured at the indicated time points. n = 5 biologically independent mice. Data are mean ± s.d. *p* values are shown.

(**P-U**) The indicated U2OS/MTX300 stable cells were subcutaneously injected into mice. **P and S**. Tumor size was measured at the indicated time points, and tumors were dissected at the endpoint. **Q and T**. Representative images of subcutaneous xenograft tumors. **R and U**. Tumor weight was measured at the endpoint. n = 5 biologically independent mice. Data are mean ± s.d. *p* values are shown.

(V) The indicated U2OS stable cells were analyzed by Western blotting.

(W) Representative immunohistochemical images of low and high protein levels of L3MBTL2 in osteosarcoma tissues.

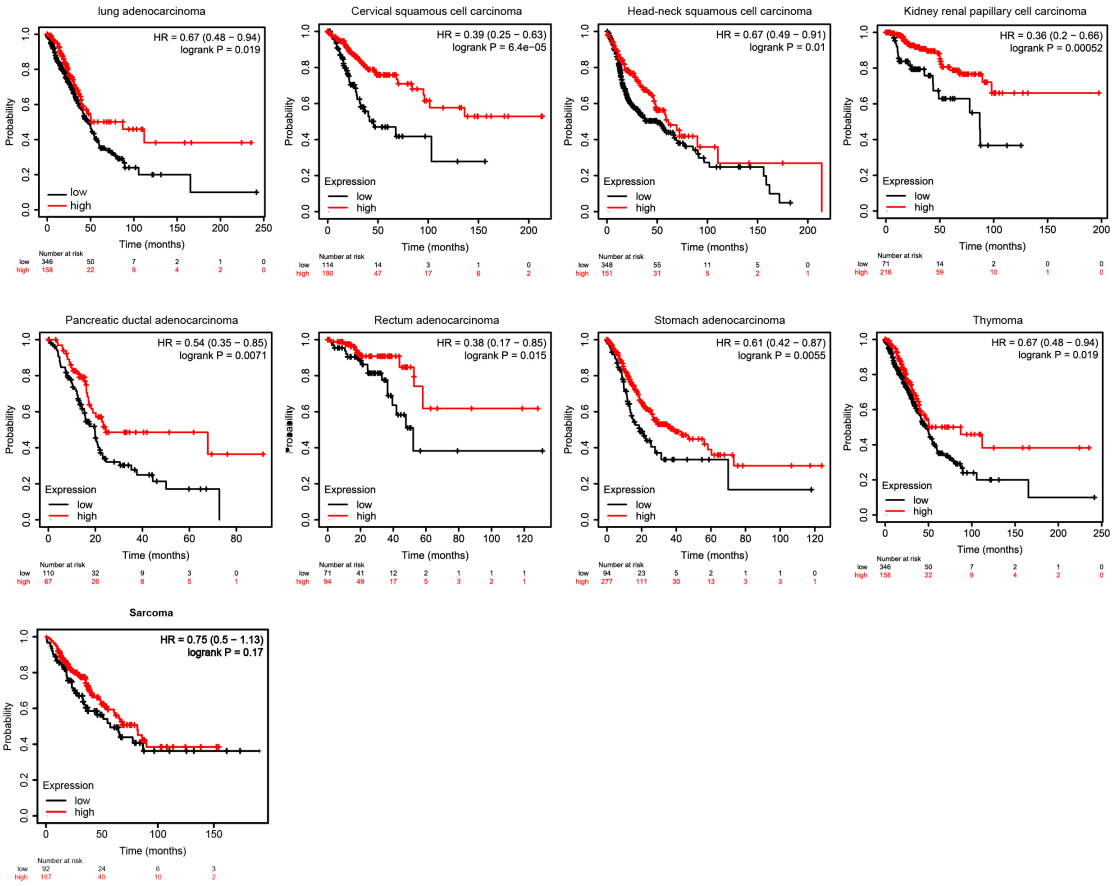

Fig. S2. High expression of L3MBTL2 is associated with favorable prognosis in pan-cancer

For correlation analysis between L3MBTL2 and prognosis, Kaplan-Meier plotting and log-rank test were done using a publicly accessible online tool KM Plotter (http://kmplot.com). Patients were divided into two classes based on auto select best cutoff.

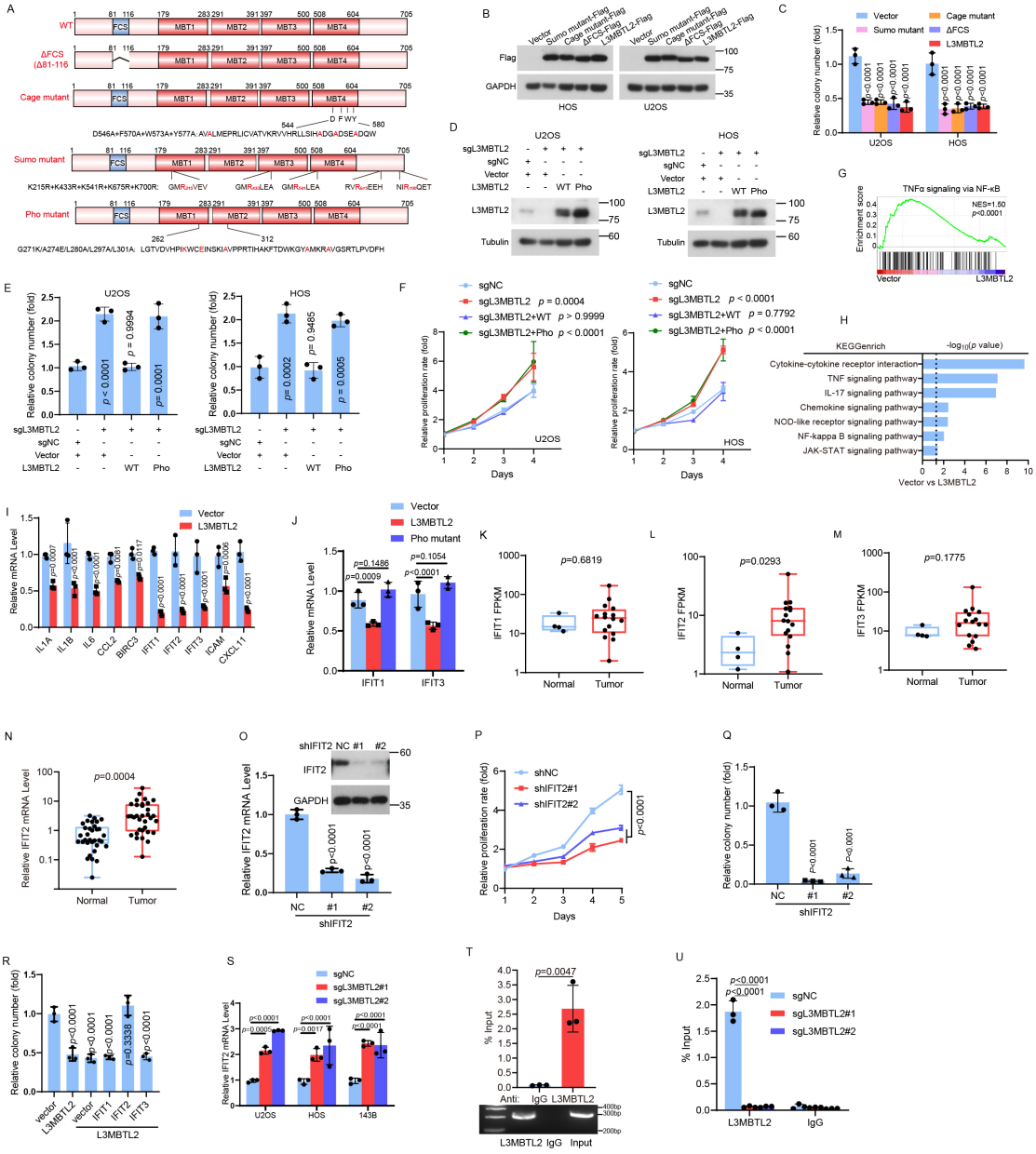

Fig. S3. L3MBLT2 exerts tumor-suppressive function via transcriptional repressing IFIT2, which is dependent on its pho-binding pocket

(**A**) Schematic description of the L3MBTL2 domains and mutants.

(**B**) The indicated stable cells were analyzed by Western blotting.

(**C**) Colony formation assay was performed for the indicated stable cells. The colony numbers per field were counted.

(**D**) The indicated stable cells were analyzed by Western blotting.

(**E**) Colony formation assay was performed for the indicated stable cells. The colony numbers per field were counted.

(**F**) Cell viability of the indicated stable cells was measured by MTT assay at the indicated

time points.

(**G**) Gene set enrichment analysis for gene expression profiles in 143B cells stably expressing vector or L3MBTL2.

(**H**) KEGG enrichment pathways analysis for gene expression profiles in 143B cells stably expressing vector or L3MBTL2.

(**I, J**) The relative indicated gene mRNA levels were normalized to the GAPDH levels in the indicated 143B stable cells as determined by RT-qPCR.

(**K-M**) The statistical results of IFIT1 (**K**), IFIT2 (**L**) and IFIT3 (**M**) mRNA levels from our RNA-seq data for 16 osteosarcoma and 4 normal muscle tissues.

(**N**) The IFIT2 mRNA levels were normalized to the GAPDH levels in the paired osteosarcoma and normal tissues (n=33) as determined by RT-qPCR.

(**O**) The IFIT2 mRNA and protein levels in the indicated 143B stable cells were determined by RT-qPCR and Western blotting, respectively.

(**P**) Cell viability of the indicated 143B stable cells were measured by MTT at the indicated time points.

(**Q, R**) Colony formation assay was performed for the indicated 143B stable cells. The colony numbers per field were counted.

(**S**) The IFIT2 mRNA levels were normalized to the GAPDH levels in the indicated stable cells as determined by RT-qPCR.

(**T**) The ChIP-qPCR assay was performed in U2OS cells using anti-L3MBTL2 antibody or IgG antibody, as indicated.

(**U**) ChIP-qPCR analysis of L3MBTL2 occupancy at IFIT2 promoter region in the indicated U2OS stable cells.

Data in **B, D**, **O and U** are representative of n = 3 biologically independent experiments

Data in **C, E, F**, **I, J and O-U** are mean ± s.d. of n = 3 biologically independent experiments. *p* values are shown.

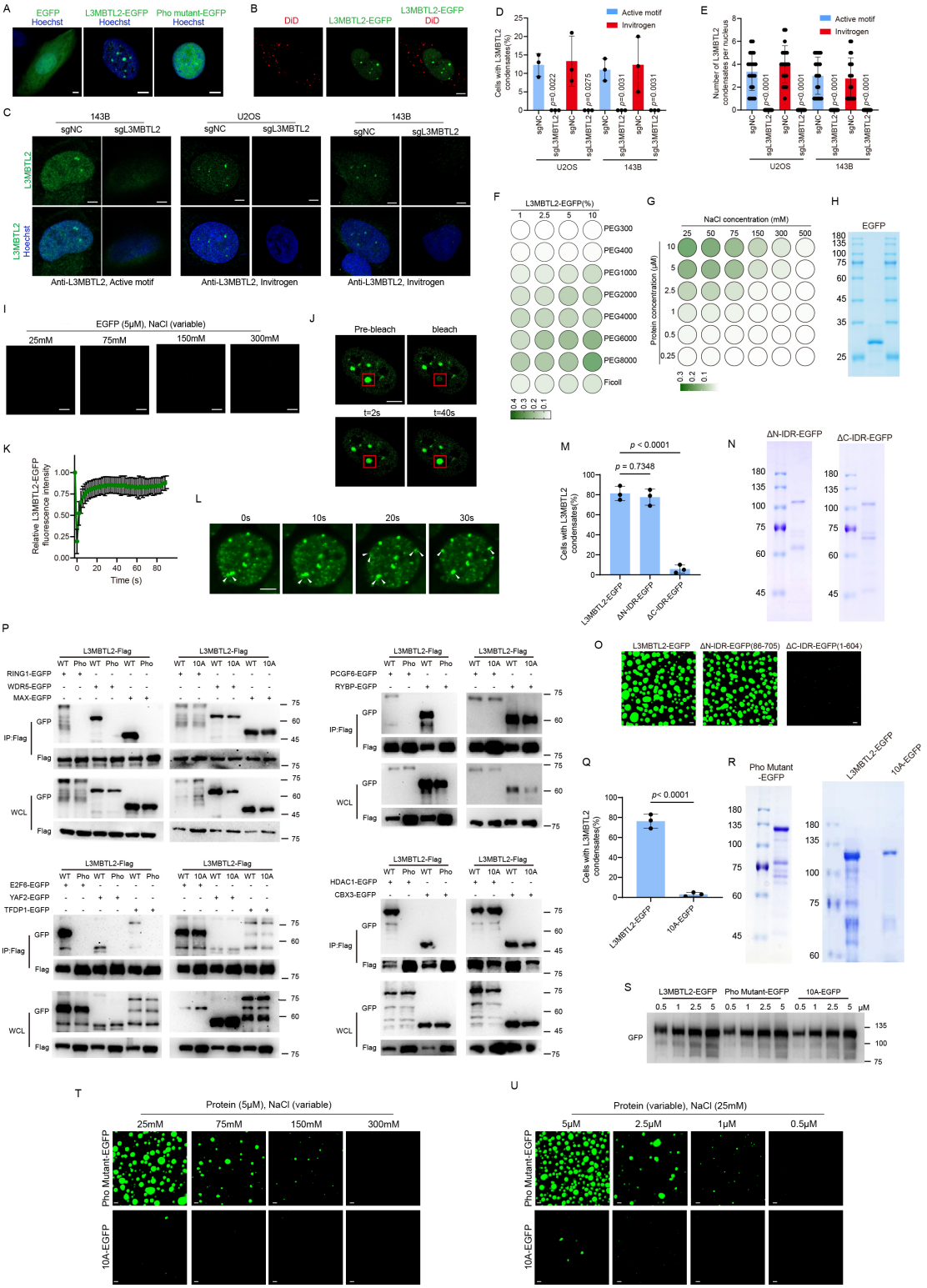

Fig. S4. Both Polybasic region and pho- binding pocket of L3MBTL2 are required for formation of L3MBTL2-induced condensates

(**A**) Representative fluorescence microscopy images in U2OS cells transfected with the indicated plasmids. Scale bar, 5μm.

(**B**) Live-image of U2OS cells transfected with L3MBTL2-EGFP and stained with DiD.

Scale bar, 5μm.

(**C**) Representative images of immunofluorescence staining for endogenous L3MBTL2 using the indicated antibodies against L3MBTL2 in the indicate stable cells. Green: L3MBTL2. Blue: Hoechst. Scale bar, 5μm.

(**D**) Percentage of n=100 cells with L3MBTL2 condensates in the indicated stable cells from **Fig. 3A** and **Fig. S4C**. Data are mean ± s.d. of n = 3 biologically independent experiments. *p* values are shown.

(**E**) Quantification of the numbers of L3MBTL2 condensate per nucleus in cells from **Fig. 3A** and **Fig. S4C**. Data are mean ± s.d. of n = 20 cells for each group. *p* values are shown.

(**F**) The purified L3MBTL2-EGFP proteins (1μM) were incubated with phase separation buffer (25 mM Tris-HCl, 1 mM DTT, pH 7.2) at 50 mM sodium chloride in the presence of increasing levels of large polymeric crowders for 5 min at room temperature. LLPS ability of L3MBTL2 under different conditions was color-coded on the basis of droplet turbidity measured at OD_{600}

(**G**)The phase diagrams of L3MBTL2 proteins with the concentration ranging from 0.25-10 μM in phase separation buffer (25 mM Tris-HCl, 1 mM DTT, pH 7.2) at the indicated concentration of sodium chloride (ranging from 25-500 mM) with 1% (w/v) PEG6000. Green dots, phase separation; white dots, no phase separation. LLPS ability of L3MBTL2 under different conditions was color-coded on the basis of droplet turbidity measured at OD_{600} when proteins were incubated with phase separation buffer for 5 min at room temperature.

(H) Coomassie blue staining of the SDS-PAGE gels with the purified EGFP proteins.

(I) Representative fluorescence microscopy images of 5 μM purified EGFP proteins in the phase separation buffer with the indicated NaCl concentration in presence of 1% (w/v) PEG6000. Experimental testing conditions: Incubation at room temperature for 1 min. Scale bar, 5 μm.

(**J**) Representative FRAP recovery images of nuclear L3MBTL2-EGFP condensates in U2OS cells transiently expressing L3MBTL2-EGFP. The red box indicates the region of photobleaching. Scale bar, 5μm.

(**K**) Quantification of fluorescence recovery of L3MBTL2-EGFP signals in live U2OS cells

transiently expressing L3MBTL2-EGFP by FRAP experiments. Data are mean ± s.d. of n = 26 cells.

(**L**) Live-images of U2OS cells transiently expressing L3MBTL2-EGFP. The arrows show representative fusion events of L3MBTL2 condensates. Scale bar, 5μm.

(**M**) Percentage of n=100 cells with L3MBTL2 condensates in the indicated cells from **Fig. 3I** and. Data are mean ± s.d. of n = 3 biologically independent experiments. *p* values are shown.

(**N, R**) Coomassie blue staining of the SDS-PAGE gels with the indicated purified recombinant proteins.

(**O**) Representative fluorescence images of 5μM WT (1-705aa), ΔN-IDR (86-705aa) or ΔC-IDR (1-604aa) in phase separation buffer with 25 mM NaCl and 1% PEG6000. Experimental testing conditions: Incubation at room temperature for 1 min. Scale bar, 5μm.

(**P**) HEK293T cells were co-transfected with the indicated plasmids, and then were lysed and analyzed by immunoprecipitation using anti-Flag followed by Western blotting. WCL: whole cell lysate.

(**Q**) Percentage of n=100 cells with L3MBTL2 condensates in the indicated cells from **Fig. 3K**. Data are mean ± s.d. of n = 3 biologically independent experiments. *p* values are shown.

(**S**) The purified L3MBTL2-EGFP, Pho mutant-EGFP or 10A-EGFP were loaded at the indicated concentration on a gel followed by Western blotting.

(**T**) Representative images of 5 μM purified Pho mutant-EGFP or 10A-EGFP in the phase separation buffer with the indicated NaCl concentration and 1% (w/v) PEG6000 for 1 min at room temperature. Scale bar, 5μm.

(**U**) Representative images of purified Pho mutant-EGFP or 10A-EGFP at the indicated protein concentration in the phase separation buffer with 25 mM NaCl and 1% (w/v) PEG6000 for 1 min at room temperature. Scale bar, 5μm.

Data in **A-C, I, J, L**, **O, P and S-U** are representative of n = 3 biologically independent experiments.

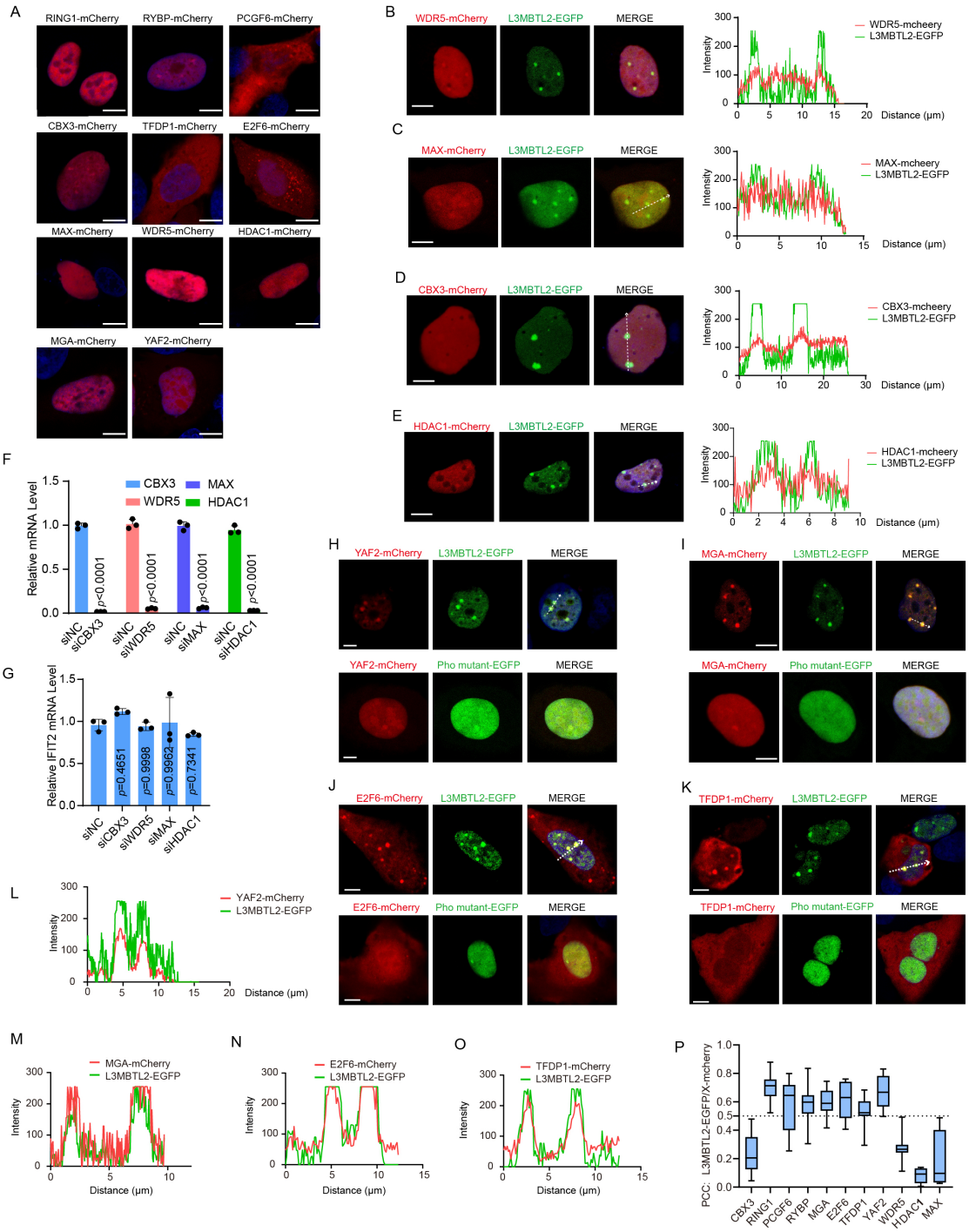

Fig. S5. L3MBTL2 selectively recruits the subunits of PRC1.6 complex to form co-condensates in osteosarcoma cells

(**A**) Representative fluorescence microscopy images of U2OS cells stably expressing vector transfected with the indicated plasmids. Hoechst 33342 was used to stain nuclei. Scale bar, 5μm.

(**B-E**) Left: Representative fluorescence microscopy images of U2OS cells co-transfected with the indicated plasmids. Scale bar, 5μm. Right: Line scan analysis of the fluorescence

intensity along the indicated line.

(**F, G**) U2OS cells were transfected with the indicated siRNA for 24 hours, and then were analyzed by RT-qPCR. The indicated mRNA levels were normalized to GAPDH levels. Data are mean ± s.d. of n = 3 biologically independent experiments. *p* values are shown.

(**H-K**) Representative fluorescence microscopy images of U2OS cells co-transfected L3MBTL2-EGFP with YAF2-mCherry (**H**), MGA-mCherry (**I**), E2F6-mcherry (**J**) or TFDP1-mCherry (**K**). Scale bar, 5μm.

(**L-O**) Line scan analysis of the fluorescence intensity along the indicated line in (**H-K)**.

(**P**) Recruitment of different PRC1.6 mCherry fusion proteins into L3MBTL2 condensates (PCC: Pearson correlation coefficient). n=13/12/12/12/9/8/13/10/6/5/4 for Ring1/PCGF6/RYBP/MGA/E2F6/TFDP1/YAF2 /WDR5/CBX3/HDAC1/MAX. Data are mean ± s.d.

Data in **A-E, H-O** are representative of n = 3 biologically independent experiments.

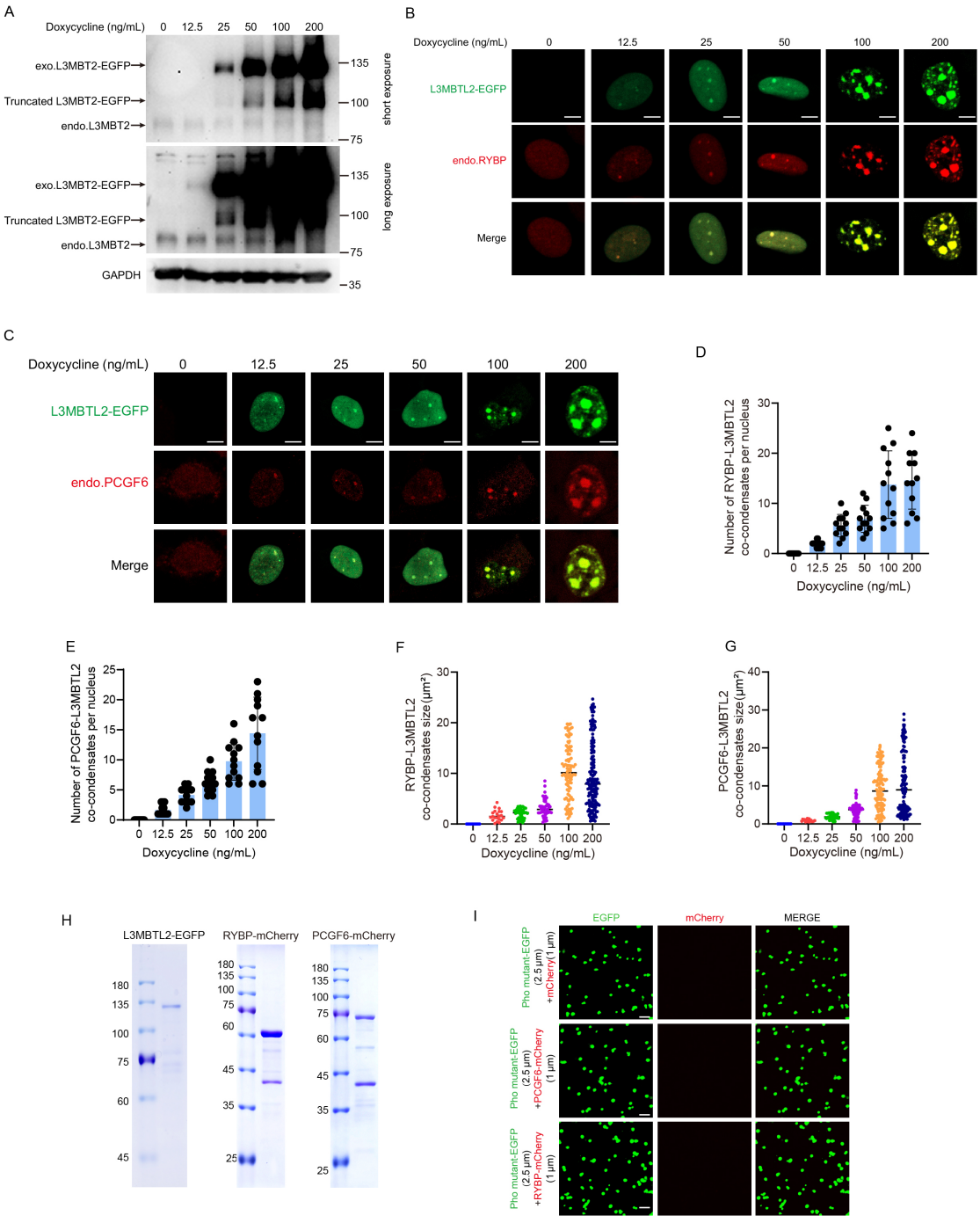

Fig. S6. L3MBTL2 forms nuclear condensates in a concentration-dependent manner

(**A**) U2OS cells stably expressing pTeton-L3MBTL2-EGFP were treated with doxycycline at the indicated doses for 24 hours, and cells were analyzed by Western blotting.

(**B, C**) Representative confocal microscopy images of U2OS cells stably expressing pTeton-L3MBTL2-EGFP incubated with doxycycline at the indicated doses for 24 hours. EGFP signals (Green) and Endogenous RYBP (**B**), PCGF6 (**C**) were shown. Scale bar, 5μm.

(**D-G**) Quantification of the number (**D, E**) and size (**F, G**) of the nuclear condensates from **B and C** by using ZEN software (version 3.7). Data are mean ± s.d. of n = 12 cells for each group. p values are shown.

(**H**) Coomassie blue staining of the SDS-PAGE gels with the indicated purified recombinant proteins.

(**I**) Representative images of the indicated proteins in the phase separation buffer with 25 mM NaCl for 1 min at 25°C. Scale bar, 5 μm.

Data in **A-C** and **I** are representative of n = 3 biologically independent experiments.

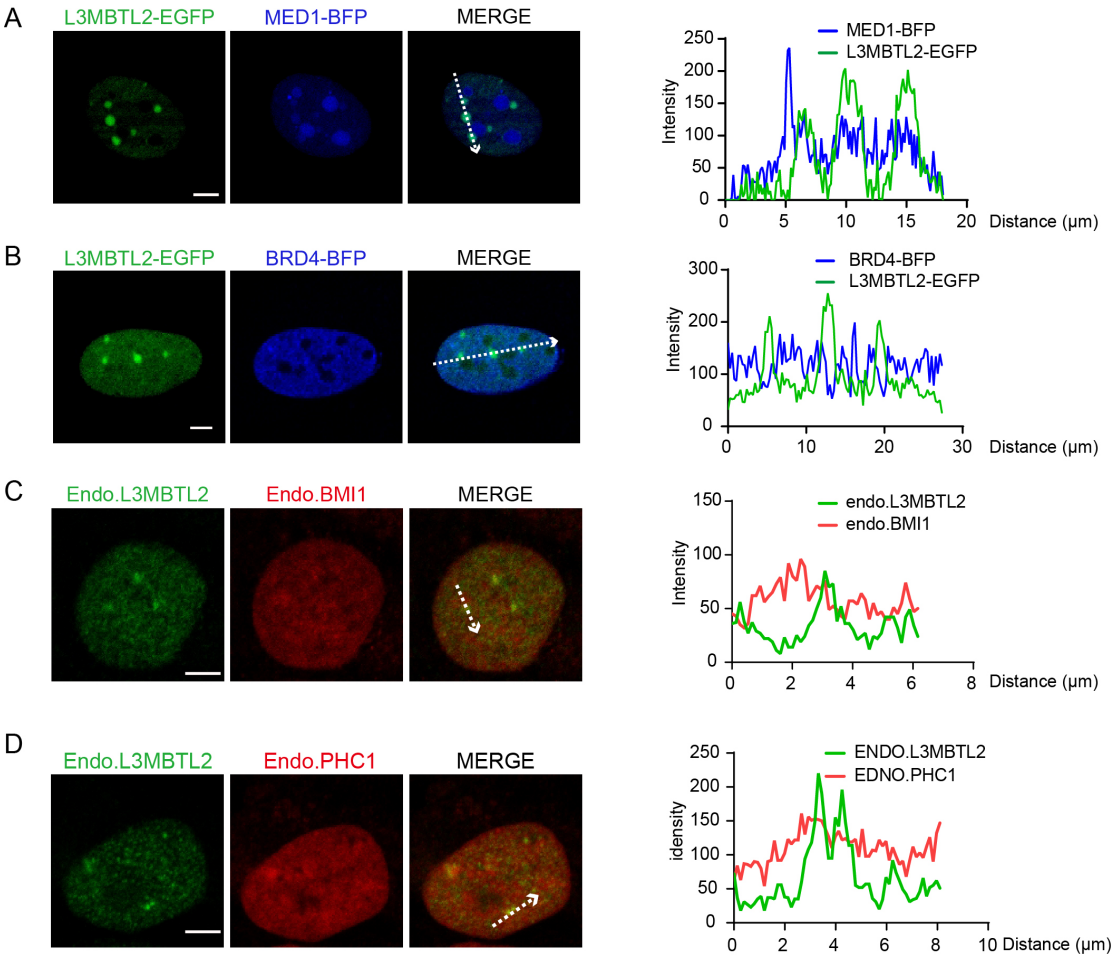

Fig. S7. Canonical PRC1 subunits and transcriptional activators were not involve in the L3MBTL2 condensates

(**A-D**) Left: Representative fluorescence microscopy images of U2OS cells co-transfected with the indicated plasmids. Scale bar, 5μm. Right: Line scan analysis of the fluorescence intensity along the indicated line. Data are representative of n = 3 biologically independent experiments.

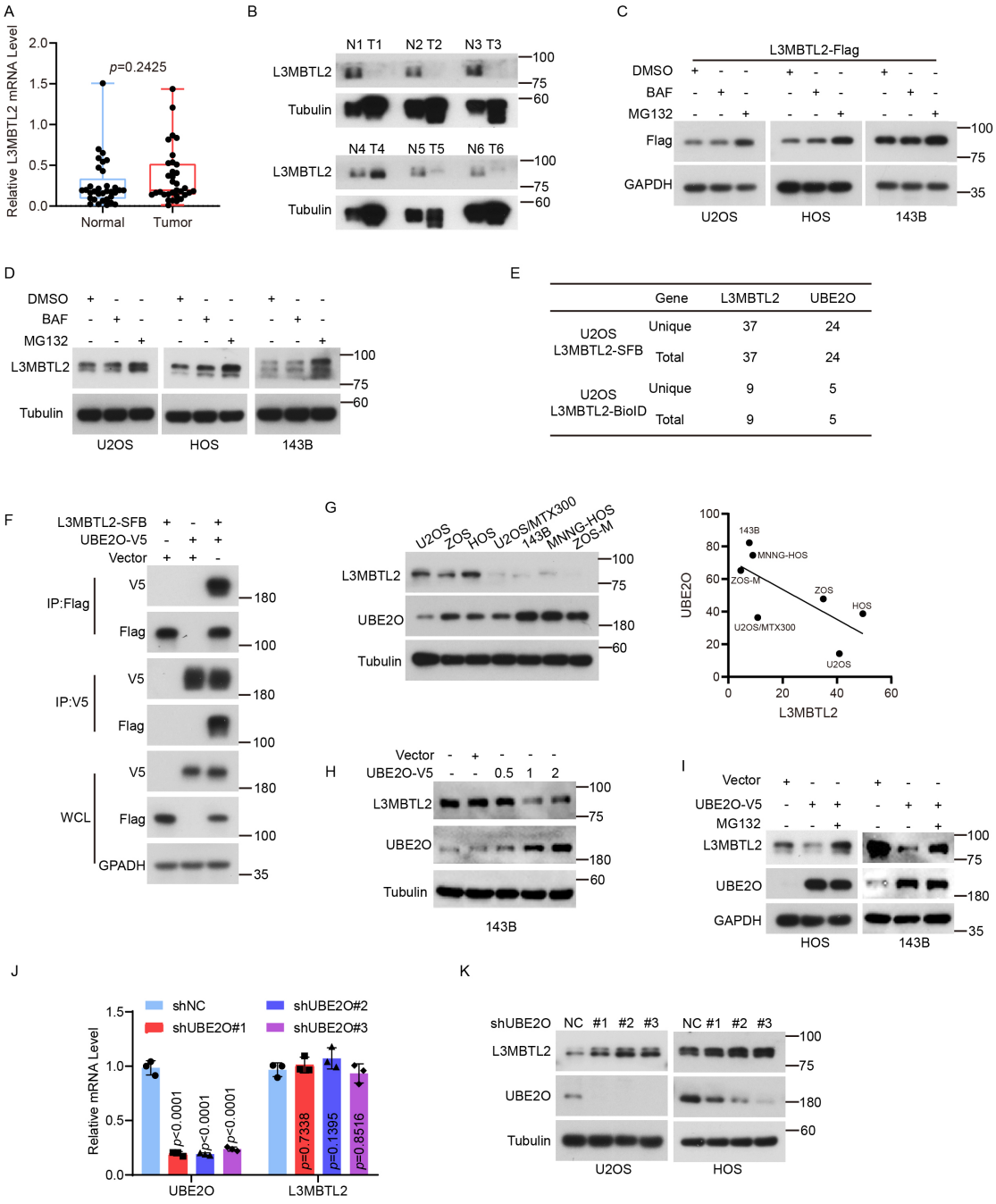

Fig. S8. UBE2O is an E3 ligase responsible for degradation of L3MBTL2

(**A**) L3MBTL2 mRNA levels were normalized to GAPDH levels in the paired osteosarcoma and normal tissues as determined by RT-qPCR. n=33, Data are mean ± s.d. *p* values are shown.

(**B**). Six paired normal and osteosarcoma tissues were lysed and analyzed by Western blotting.

(**C**) The indicated osteosarcoma cells transfected with L3MBTL2-Flag for 40 hours were incubated with DMSO, MG132 or bafilomycin (BAF) for 8 hours, and then were analyzed

by Western blotting.

(**D**) The indicated osteosarcoma cells were treated with DMSO, MG132 or bafilomycin (BAF) for 8 hours, and then were analyzed by Western blotting.

(**E**) Table of the unique and total peptide numbers for UBE2O and L3MBTL2 detected by MS using the indicated stable cells.

(**F**) HEK293T cells were co-transfected with the indicated plasmids, and then were lysed and analyzed by immunoprecipitation using anti-Flag or anti-V5 beads followed by Western blotting. WCL: whole cell lysate.

(**G**) Left: The indicated osteosarcoma cell lines were analyzed by Western blotting. Right: The correlation scatter plots were shown based on the protein levels of L3MBLT2 and UBE2O. The relative intensities of L3MBTL2 and UBE2O were quantified with ImageJ software and normalized with Tubulin.

(**H**) 143B cells were transfected with increasing amounts of UBE2O-V5 plasmids for 48 hours, and then were analyzed by Western blotting.

(**I**) The indicated osteosarcoma cells transfected with vector or UBE2O-V5 for 40 hours were incubated with or without MG132 for 8 hours, and then were analyzed by Western blotting.

(**J**) The indicated mRNA levels were normalized to GAPDH levels in the indicated 143B stable cells as determined by RT-qPCR. Data are mean ± s.d. of n = 3 biologically independent experiments. *p* values are shown.

(**K**) The 143B indicated stable cells were analyzed by Western blotting.

Data in **B-D, F-I** and **K** are representative of n = 3 biologically independent experiments.

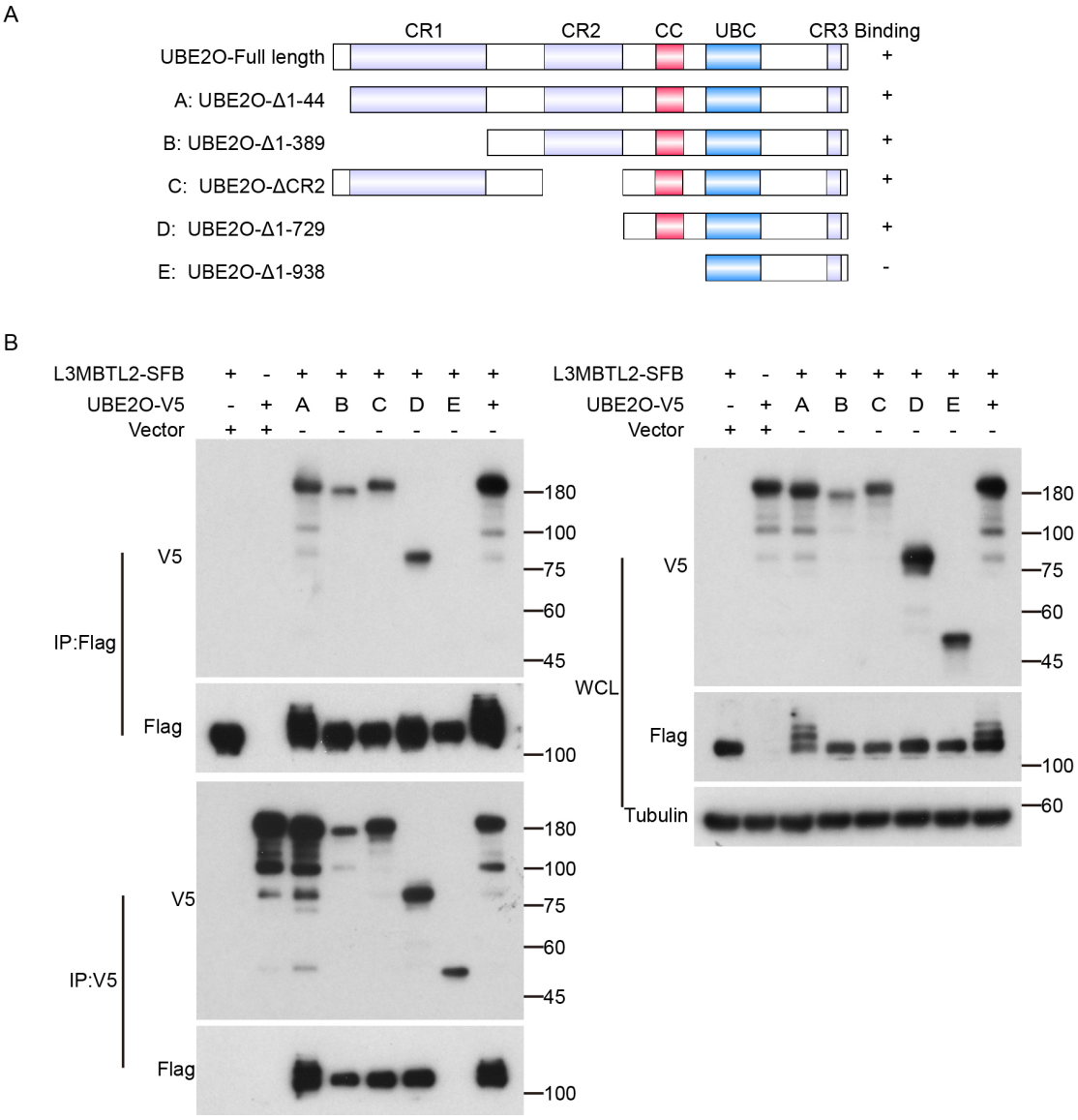

Fig. S9. CC domain of UBE2O is critical for binding to L3MBTL2

(**A**) Schematic illustration of UBE2O-V5 truncations used for co-IP assays with L3MBT2-SFB.

(**B**) 293T cells were co-transfected with the indicated plasmids, and then were lysed and analyzed by immunoprecipitation using anti-Flag or anti-V5 beads followed by Western blotting. Data are representative of n = 3 biologically independent experiments.

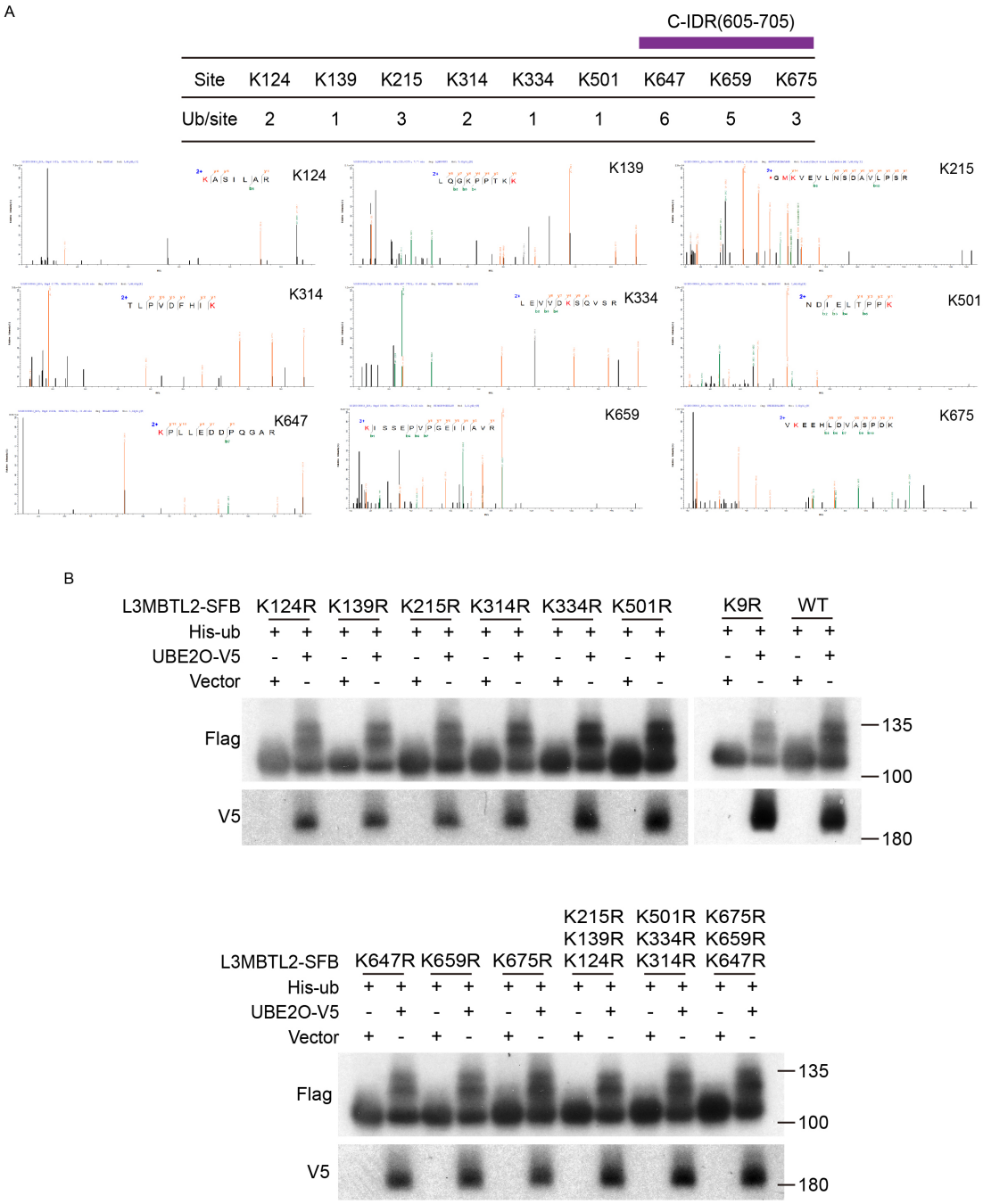

Fig. S10. UBE2O catalyzes the multi-monoubiquitination of L3MBTL2

(**A**) Ubiquitination events detected by MS.

(**B**) 293T cells were co-transfected with the indicated plasmids, and then were analyzed by Western blotting. Data are representative of n = 3 biologically independent experiments.

Supplementary Table S1-S12 (Separate files)

Table S1. The statistics of the CRIPSR screening results in U2OS cells.

Table S2. The statistics of the CRIPSR screening results in HOS cells.

Table S3. RNA-seq analysis result of 143B cells expressing vector or L3MBTL2 wild type**.**

Table S4. RNA-seq analysis result of 143B cells expressing L3MBTL2 wild type or Pho mutant.

Table S5. RNA-seq analysis result of 143B cells expressing vector or Pho mutant.

Table S6. The differential peaks from CUT&TAG results between 143B cells stably expressing L3MBTL2-WT and the 10A mutant.

Table S7. L3MBTL2 binding partners identified by tandem affinity purification and mass spectrometry.

Table S8. L3MBTL2 binding partners identified by Bio-ID and mass spectrometry.

Table S9. L3MBTL2 ubiquitination sites identified by mass spectrometry analysis.

Table S10. Oligonucleotides sequences summary.

Table S11. Antibodies and reagents.

Table S12. Human osteosarcoma tissues and the IHC scores of L3MBTL2 and UBE2O.